INT. J. REMOTE SENSING, 1994, VOL. 15, NO. 14, 2917–2930

Effect of scattering mechanisms on polarimetric features of crops and trees

P. DE MATTHAEIS, G. SCHIAVON and D. SOLIMINI

Dipartimento di Ingegneria Elettronica, Università Tor Vergata,
Via della Ricerca Scientifica, 00133 Roma, Italy

Abstract. This paper discusses selected features of backscatterig data collected in summer 1989 at *C*, *L* and *P* band over the Dutch Flevoland test site by the NASA/JPL airborne polarimetric SAR within the MAESTRO 1 Campaign. The dependence of the response of microwave active sensors on the different types and conditions of soils, crops and trees is analysed on the basis of polarization responses (or signatures), backscattered powers at relevant polarizations and correlation coefficients. The scattering mechanisms that appear to be effective in controlling the copolar and cross-polar radar responses of different vegetation types at the three radar frequencies are discussed too.

1. Introduction

Recent airborne campaigns are providing multi-frequency radar data of noticeable value to identify the soil and vegetation parameters which have a dominant influence on the intensity and polarization properties of backscattering from areas devoted to agricultural practices and to forestry. The collected data also offer the means of evaluating the sensitivity of the radar responses to these parameters, with a view to devising and tuning retrieval procedures and algorithms. A preliminary step is the understanding of the acting scattering mechanisms and the assessment of how their relative contributions change with the characteristics of the terrain and of the covering vegetation.

In 1989 the European Space Agency (ESA) and the EC Joint Research Centre (JRC), Ispra, supported the deployment of the NASA/JPL airborne multi-band synthetic aperture polarimetric radar (AIRSAR) (Held *et al.* 1988) for the remote sensing campaign named MAESTRO 1 over several test sites in Europe (Churchill and Attema 1991). The polarimetric capability of the AIRSAR provides the opportunity of exploiting the full backscattering matrix of the imaged surface. From the five independent quantities contained in the matrix, other representations of backscatter can be derived, which, depending on the circumstances, can display distinctly some peculiarities of the scattering behaviour of the surface. In the following, we shall consider the polarization responses (or 'signatures'), the backscattering coefficients σ^0 at relevant states of polarization (such as right- and left-circular), and the complex correlation coefficient. The scattering features contain imprinting by the surface type, resulting from the different mechanisms of interaction with the electromagnetic waves. An identification of these mechanisms is attempted and some of their salient effects are discussed, also with reference to theoretical model simulations.

2. Data analysis

The measurements were carried out in the morning of 16 August 1989 over the Dutch Flevoland site. The radar imaged three areas at *P*, *L* and *C* band simultaneously: an agricultural site (Flevopolder) and two forest sites (Horsterwold and

Speulderbos). For the detailed data analysis we selected 16 fields (with wheat, sugarbeet, potatoes, corn and bare soil of different roughness) within the Flevopolder site and 11 forest areas (with poplar, maple, ash, beech, oak and Scots pine trees) within the other two sites, for which intensive ground data were available, collected by a team from the Wageningen Agricultural University (Droesen *et al.* 1990). On these selected areas the incidence angle ranged from about 29° to 51°.

A (relative) calibration of amplitude and phase among the polarization channels (i.e. *HH*, *HV*, *VH* and *VV*) and a global absolute calibration were needed to transform the radar output data into maps of calibrated backscattering features. To this end, we essentially followed the technique proposed by van Zyl (1990) and Zebker and Lou (1990), aiming at basing the calibration procedure on natural (extended) targets in addition to corner reflectors.

For the relative phase calibration, four areas of sufficient extension (including not less than 180 pixels) showing rather uniform amplitude and phase backscattering properties were chosen in the near range of the Flevopolder image (corresponding to angles of observation $\theta \cong 20°$). The measured phase was then corrected by using its average over the four areas, for which the phase difference between *HH* and *VV* returns is expected to be close to zero. The obtained results were validated against those estimated from the response of four corner reflectors deployed on the fields of the same Flevopolder area. The phase factors determined from the extended targets were quite close to those obtained from the corner reflectors at *C* and *L* band (within 2° and 5°, respectively), but a less satisfactory agreement (about 20°) was obtained at *P* band. To estimate the cross talk parameters, 16 areas uniformly distributed in range were selected, for which the phase difference between *HH* and *VV* return was less than 40° and a single mechanism of scattering was presumably present. Radar data were then corrected for the cross-talk by using piecewise linear interpolations of the real and imaginary parts of the estimated cross-talk parameters as functions of the incidence angle. Finally, the imbalance between channels was corrected by using the responses of the four trihedral corner reflectors located in the Flevopolder area (Zebker and Lou 1990). The effects of the mentioned calibration steps were assessed by observing the modifications they introduced in the co- and cross-polar responses of the corner reflectors. At the end of the calibration procedure, their measured polarization responses at *C* and *L* band were almost indistinguishable from the theoretical ones (van Zyl and Ulaby 1990), whereas a slight distortion was still apparent at *P* band.

The last step of our calibration procedure concerned the absolute radiometric calibration. To this end, the measured backscattering cross-sections of the mentioned corner reflectors were compared with their theoretical ones, deduced from sizes and orientations with respect to the NASA aircraft (Groot 1991, private communication). The available data referred to corner reflectors deployed on the Flevopolder subsite, whereas calibrators were not available in Horsterwold or in Speulderbos. To calibrate the data taken on these forest areas, constant-azimuth stripes belonging to both Flevopolder and Horsterwold images and to both Horsterwold and Speulderbos were identified, and correcting factors were calculated in order that areas which were shared by two images had the same σ^0 and phase at each frequency and polarization. It was noted that the factors did not change appreciably with polarization at *C* and *L* band, whereas at *P* band different correcting factors were needed for σ^0_{HH}, σ^0_{VV} and σ^0_{HV}. At the end of the radiometric calibration, we expect to obtain good results at *C* band, where the sizes of the corner

reflectors in terms of wavelength are relatively large, but progressively poor results at the lower frequencies. In particular, the corner reflectors deployed in the Flevopolder area were not large at P band, so that the ratio between their backscattering and the one contributed by the terrain was not sufficiently high to guarantee the accuracy of the absolute radiometric calibration.

After calibration, the elements of the Stokes matrices at the three frequencies were computed and averaged over the pixels belonging to each of the 27 selected fields and forest areas. Then polarization responses, amplitude and phase histograms (de Matthaeis *et al.* 1992 a), co- and cross-polar backscattering coefficients, and correlation coefficients were determined for the agricultural fields and for the various kinds of woodland present in the selected parts of the imaged areas. Unfortunately, RF interference took place at P band while data were being taken over the Horsterwold subsite. Therefore, some of the P band results for this forest site are considered of limited reliability and will not be presented.

2.1. *Scattering parameters*

Further averaging was performed on the calibrated backscattering data to obtain a single Stokes matrix for each type of surface, i.e., 'smooth' and 'rough' bare soil, wheat, sugarbeet, normal and defoliated corn, poplar, ash, oak, beech, maple and Scots pine. In table 1 we report the mean values of σ^0_{HH}, σ^0_{VV}, σ^0_{HV}, $\Delta\phi_{VV}=\phi_{HH}-\phi_{VV}$ and $\Delta\phi_{HV}=\phi_{HH}-\phi_{HV}$ for the mentioned homogeneous types of surface. As 'smooth' bare soil we chose two fields having r.m.s. surface heights $\delta=5$ mm and 11 mm and mean exponential correlation lengths $L=37$ mm and 43 mm, respectively, while the 'rough' bare soil had $\delta=16$ mm and 19 mm and $L=39$ mm and 45 mm, respectively. We keep the two fields of corn separated (in the following called 'normal' and 'defoliated'), since one of them had been particularly damaged by a hail storm, and consisted essentially of the stalks and of small portions of leaf ribs. Details on the measured parameters, methodology and characteristics of the site and vegetation can be found in Droesen *et al.* (1990). Note that we omit to report those P band data which are deemed to be of questionable reliability because of the mentioned local RF interferences.

From an inspection of table 1, we remark that within the Flevopolder agricultural area and for the four considered types of crops, the values of σ^0_{HH} span a range of about 1 dB at C band, 7 dB at L band and 8 dB at P band. For vertical polarization, a similar range of variation is observed at C and P band, while it is reduced at L band. Finally, the differences in the cross-polar return among the various crops are close to the copolar ones at C and P band, whereas they increase (up to about 10 dB) at L band. A comparison between the values of σ^0 for the agricultural crops and those for the considered woodlands indicate that a small difference exists at C band for all three polarizations, the considered trees being slightly less reflective than sugarbeet, potato and corn. At L band, some types of trees (Scots pine, in particular), exhibit both co- and cross-polar responses moderately higher than those of the crops, whereas the measurements at P band (especially σ^0_{HH} and σ^0_{HV}) discriminate distinctly between crops and trees. It is interesting to note that the overall ranges of variation of the values of σ^0 at the various frequencies are consistent with the measurements reported by Dobson *et al.* (1992) for clearcuts and coniferous forest. The phase difference $\Delta\phi_{VV}$ is practically independent of the type of surface at C band, while at L band $\Delta\phi_{VV}$ of defoliated corn and maple differs markedly from that of the other vegetation types, probably because of an even

Table 1. σ^0_{HH}, σ^0_{VV}, σ^0_{HV}, $\Delta\phi_{VV}=\phi_{HH}-\phi_{VV}$ and $\Delta\phi_{HV}=\phi_{HH}-\phi_{HV}$ *measured at P, L and C band for different types of surfaces.*

		C band					*L* band					*P* band				
Type of surface	θ	σ^0_{HH}	σ^0_{VV}	σ^0_{HV}	$\Delta\phi_{VV}$	$\Delta\phi_{HV}$	σ^0_{HH}	σ^0_{VV}	σ^0_{HV}	$\Delta\phi_{VV}$	$\Delta\phi_{HV}$	σ^0_{HH}	σ^0_{VV}	σ^0_{HV}	$\Delta\phi_{VV}$	$\Delta\phi_{HV}$
Smooth bare soil	35°, 50°	−11·9	−12·0	−21·8	−15°	−52°	−16·6	−13·7	−28·4	−14°	20°	−21·7	−18·3	−26·4	7°	−167°
Rough bare soil	29°, 44°	−8·8	−9·1	−18·0	−3°	−42°	−11·6	−10·9	−21·5	−16°	−145°	−15·5	−12·7	−23·8	4°	−109°
Wheat	33°, 51°	−9·0	−10·5	−16·6	−22°	−126°	−15·2	−13·3	−24·2	−32°	−77°	−20·0	−16·0	−26·0	7°	−90°
Sugarbeet	34°, 51°	−7·9	−8·0	−15·4	0°	21°	−11·8	−12·6	−20·2	−10°	59°	−12·4	−11·1	−23·5	−47°	−121°
Potato	35°, 43°	−8·2	−8·1	−15·0	5°	−4°	−9·1	−9·0	−14·6	6°	7°	−14·0	−13·9	−19·6	−32°	126°
Corn	45°	−8·9	−9·7	−15·8	1°	−153°	−9·5	−10·6	−17·3	11°	100°	−13·0	−11·9	−19·6	−10°	97°
Defoliated corn	38°	−8·9	−10·4	−15·9	−13°	−119°	−8·6	−10·7	−17·6	132°	178°	−12·9	−9·1	−17·8	77°	156°
Poplar	39°−48°	−9·6	−11·4	−16·4	−10°	157°	−9·7	−10·1	−14·7	5°	3°	*	*	*	*	*
Ash	48°	−9·8	−11·5	−17·4	1°	109°	−9·5	−10·6	−16·7	41°	−129°	*	*	*	*	*
Oak	44°	−9·7	−10·4	−15·8	−5°	145°	−9·1	−8·9	−13·6	−1°	−175°	−5·5	−5·3	−11·4	100°	−75°
Beech	43°, 46°	−10·6	−10·9	−16·4	−3°	−2°	−8·9	−8·0	−13·0	11°	−28°	−5·8	−4·1	−9·1	77°	64°
Maple	41°	−9·4	−11·7	−17·8	−4°	152°	−8·7	−10·2	−16·9	114°	47°	*	*	*	*	*
Scots pine	47°	−10·1	−12·1	−16·2	−2°	158°	−7·0	−6·9	−11·6	5°	92°	−2·7	−4·6	−8·5	88°	−143°

(*) affected by RF interference

bounce scattering mechanism, in agreement with the observation that, correspondingly, $\sigma^0_{HH} > \sigma^0_{VV}$ (van Zyl 1989). The values of $\Delta\phi_{VV}$ at P band are relatively low for bare soil, wheat and normal corn, increase for potato and sugarbeet and approach or exceed 90° in the case of defoliated corn and trees. Finally, the mean values of $\Delta\phi_{HV} = \phi_{HH} - \phi_{HV}$ appear to behave erratically, without relation to the type of surface. Indeed, we have observed that the corresponding phase histograms, not reported here, are rather flat.

2.2. *Polarization responses*

The polarization responses (van Zyl *et al.* 1987) of the imaged agricultural and forest areas for which ground data are available, were generated for three radar frequencies. The features displayed by the plots contain the imprinting by the intervening scattering mechanisms (surface or volume scattering, multiple bouncing, etc.), which combine to yield the global co- and cross-polar backscattering for the various polarization states. Observed polarization responses of glacial moraines, bare soil, swamp areas, shrubs, crops and forest have been reported and analysed in recent years (Zebker *et al.* 1987, Evans *et al.* 1988, Durden *et al.* 1989, Mo *et al.* 1990, Skriver and Gudmandsen 1992, Forster *et al.* 1992, de Matthaeis *et al.* 1992 b). Here we present the copolar polarization responses of three types of agricultural fields and attempt to highlight the relative role of the crop morphology and of the underlying soil, by discussing the displayed features.

In figure 1 the P band copolar responses of a relatively smooth bare soil field, a potato field and the defoliated corn field are reported, together with the corresponding responses observed at L band. The P band bare soil copolar response peaks near VV polarization, while the maximum at L band is slightly less pronounced, in accordance with rough surface scattering theory. Apart from periodic ridges, the terrain below the potato canopy was slightly smoother than the bare soil field and had almost the same moisture content. However, at P band the polarization signature displays a weak maximum around VV and a remarkable pedestal, which is characteristic of volume scattering (Tsang and Ding 1991), thus giving an indication that the contribution by the succulent vegetation is appreciable at this low radar frequency. The corresponding L band response has the maximum appreciably displayed from the VV polarization. This feature is found in the case of a short cylindrical scatterer neither horizontal nor vertical (van Zyl and Ulaby 1990) and, indeed, an indication that the stems of the plants could depart from their natural uniform azimuthal distribution is given by Groot *et al.* (1992). The effect of the periodicity of the crop, planted on ridges, should also be considered, as discussed by Ray *et al.* (1991). Striking differences between P and L band responses are apparent for the field of defoliated corn. At the lower frequency, a sharp maximum peaks near VV polarization, while at L band the VV maximum is weak and distinctly lower than the one at HH. For both frequencies, the mean phase difference $\Delta\phi_{VV}$ is considerably high (table 1) and we have observed that its histograms peak towards π, thus suggesting an even-bounce scattering mechanism. Theoretical model results (Ferrazzoli and Guerriero 1994) point out that for a canopy of vertical cylinders simulating corn stalks, the dependence of backscattering intensity on polarization is set by a balance between scattering from the stalks, attenuation by the canopy and reflection from the ground. At L band, the corn stalks effectively scatter downward both vertical and horizontal polarizations, so that the attenuation by the canopy and the upward reflection from the ground, both of which damp the VV return, cause

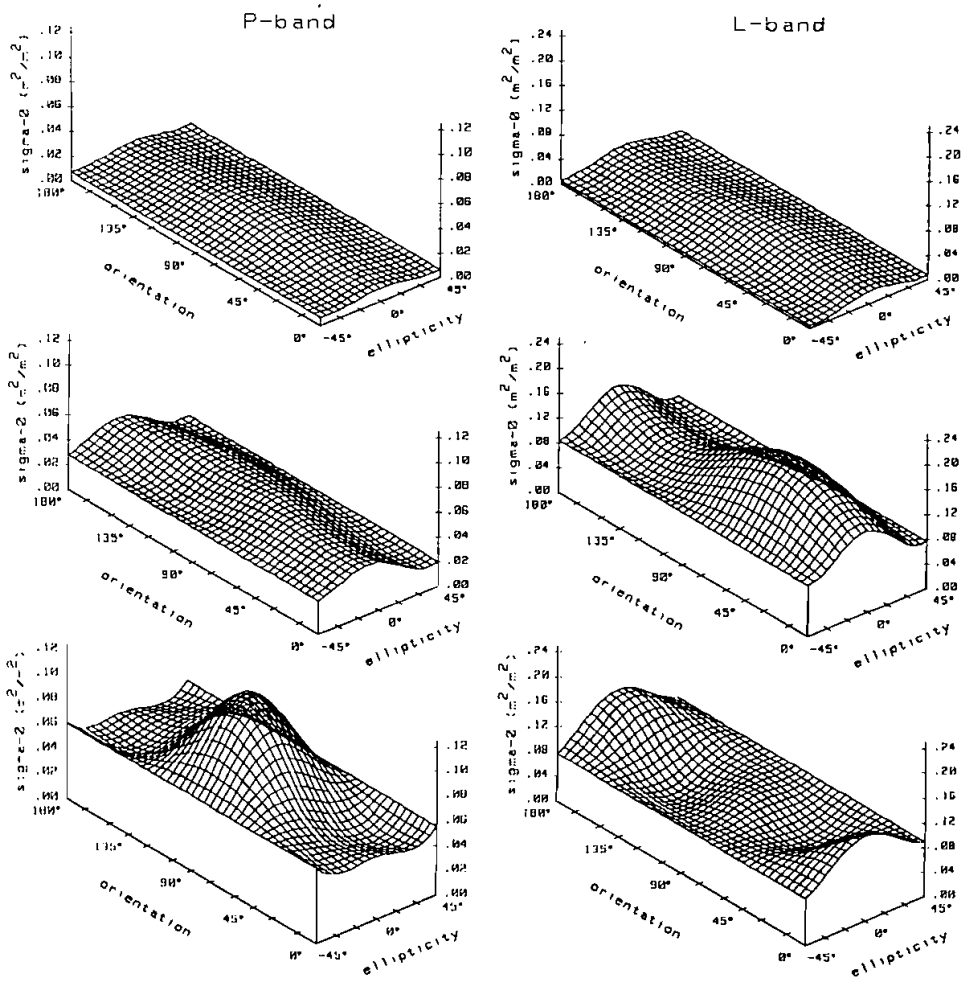

Figure 1. Polarization responses observed at *P* and *L* band for bare soil (top), potato (middle) and defoliated corn (bottom).

HH backscatter to prevail. At *P* band, the cylinders become relatively thin, so that vertical polarization is scattered appreciably more than the horizontal one and, although canopy attenuation and the ground reflection coefficient still act to reduce the vertically polarized return, the balance results in a higher *VV* backscattering.

2.3. *Backscattering and correlation coefficients*

The scattering parameters reported in table 1 contain the basic information on the peculiar scattering properties of the various types of surface. Other quantities, including phase standard deviation, amplitude ratios and correlation coefficients, have also been considered for a number of applications (Cumming *et al.* 1991, Durden *et al.* 1991, Freeman *et al.* 1991, French *et al.* 1991, van Zyl *et al.* 1991, Groot *et al.* 1992). The purpose of this section is to discuss how the various electromagnetic scattering mechanisms can be highlighted from simple representations of the radar data on selected two-parameter planes. The interpretation we

give of the observed patterns is in general consistent with the results of several theoretical models (Ulaby *et al.* 1990, Chauhan *et al.* 1991, McDonald *et al.* 1991, Zebker *et al.* 1991, Karam *et al.* 1992), and, in particular, is supported by results of simulations carried out by the Tor Vergata multiple scattering model (Ferrazzoli *et al.* 1991, Ferrazzoli and Guerriero 1994).

A straightforward approach represents the radar data of the single fields and forest stands on the plane of the linearly polarized co- and cross-polar backscattered powers, i.e. σ^0_{VV} or σ^0_{HV} vs. σ^0_{HH} (figures 2 and 3, for L band). Although the effects of the different scattering mechanisms are interweaved, different regions can be roughly identified in the plane σ^0_{VV} σ^0_{HH}, according to the mechanisms that tend to prevail in each of them. A large region, about 8 dB wide and characterized by $\sigma^0_{VV} > \sigma^0_{HH}$, contains the experimental points relative to surface scattering and includes bare soil with different roughness, and wheat, which is neither an effective scatterer nor an absorber at L band. The location of the experimental points in this region appears to be consistent with the small perturbation theory. Volume scattering from tillers, sprays and twigs (thin lossy dielectric cylinders) is prevalent both for potato fields and for poplar, beech and oak groves, for which $\sigma^0_{VV} \simeq \sigma^0_{HH}$, while a double bounce between stalk or trunk and terrain can be presumed in the region containing the experimental points for corn fields and maple and ash groves, for which $\sigma^0_{HH} > \sigma^0_{VV}$. Pine trees are located at the highest σ^0 values, with $\sigma^0_{VV} \simeq \sigma^0_{HH}$. In this case, the prevailing contribution comes from the large branches, which are weakly shielded by the crown, since they can approach the treetops. The two sugarbeet fields, for which the prevailing scattering mechanism is now from the bulk of leaves, i.e. thin lossy dielectric disks, have lower values of both σ^0_{HH} and σ^0_{VV}, and are located not far from the surface-type scattering cluster. A representation in the plane σ^0_{HV} σ^0_{HH} (figure 3) has the advantage of an increased dynamic range, but essentially maintains the same kind of clustering. The lower part of the diagram, i.e. low cross-polar backscattering,

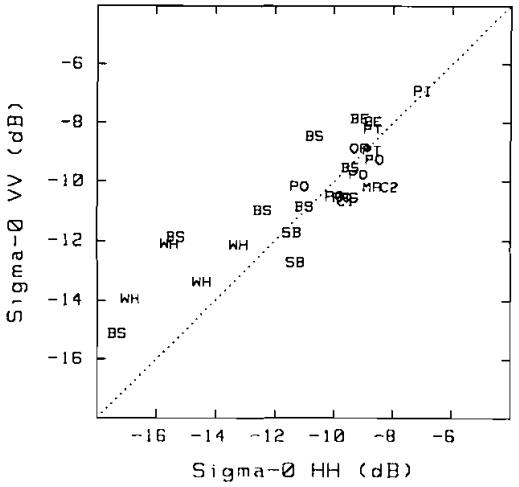

Figure 2. L band σ^0_{VV} vs. σ^0_{HH} for some agricultural fields and forest areas in the Flevoland test site. Labels denote: BE, beech; OA, oak; PI, pine; PO, poplar; MA, maple; AS, ash; C1, corn; C2, defoliated corn; PT, potato; SB, sugarbeet; WH, wheat; BS, bare soil.

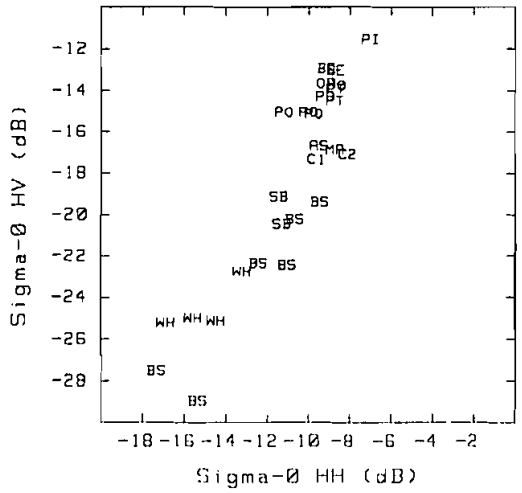

Figure 3. *L* band σ^0_{HV} vs. σ^0_{HH} for some agricultural fields and forest areas in the Flevoland test site. Labels as in figure 2.

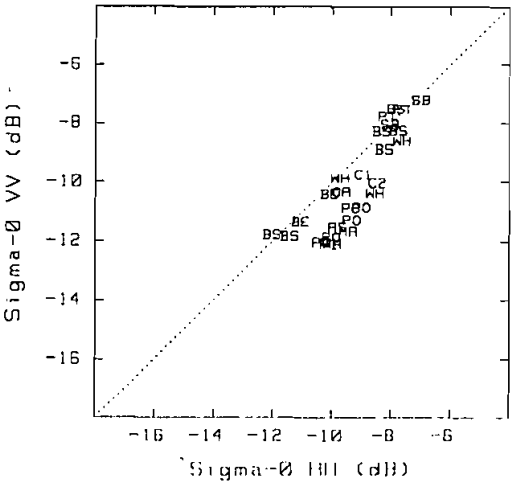

Figure 4. *C* band σ^0_{VV} vs. σ^0_{HH} for some agricultural fields and forest areas in the Flevoland test site. Labels as in figure 2.

denotes the presence of surface scattering, with bare soil and wheat fields. Sugarbeet fields have intermediate values of σ^0_{HV}, then the areas whose return is characterized by scattering from the volume of randomly oriented thin cylinders within the crown of trees (poplar, beech and oak) and in the potato canopy are found rather tightly packed together at higher cross-polar backscattering. When a stalk-terrain double-bounce effect is present, the *HH* radar return is close to the volume-scattering cluster, but depolarization (σ^0_{HV}) is lower. Finally, the cross-polar return from the pine stand is the highest, as the copolar one.

Reduced dynamic ranges are peculiar to measurements at *C* band (figure 4), for which some of the scattering mechanisms tend to be appreciably less effective. We

note that for some of the wheat fields $\sigma^0_{HH} > \sigma^0_{VV}$. This fact, in conjunction with the observed tendency of the phase difference to extend towards 180°, suggests that at this frequency a weak even-bounce scattering process between the almost vertical thin stalks of the plants and the terrain surface might be present.

P band data are reported in figure 5. The dynamic range is increased with respect to *L* band, essentially because of the noticeable separation between agricultural and forest areas. Surface scattering ($\sigma^0_{VV} > \sigma^0_{HH}$) prevails in the returns from bare soil and wheat, which at this frequency is fairly transparent. Crops with higher biomass, i.e. sugarbeet, potato and normal corn, tend to backscatter independently from polarization, while defoliated corn has the largest *VV* return. As already mentioned, the *P* band image of one of the forest areas was affected by RF interference, so that only data relative to three types of stands are reported in figure 5. Among these, pine appears to be the stand which exhibits the most appreciable trunk-terrain scattering mechanism.

The previous plots use only co- and cross-polar scattering amplitude information. Backscattering of circularly polarized waves incorporates phase information too. Figure 6 reports the measured *L*-band cross-polarized backscattering coefficients for circular polariation σ^0_{LR} vs. the co-polarized one σ^0_{RR}. Now the region of surface scattering is located in the upper-left part of the plane, i.e. with relatively high values of cross-polar return and relatively low values of the copolar one. This latter increases as the mechanisms producing volume scattering come into play and strengthen. The highest copolar return is exhibited by the trees, for which the scattering from the randomly oriented cylindrical elements in the crown combines with the moderate trunk-terrain double-bounce effect to yield either $\sigma^0_{LR} \simeq \sigma^0_{RR}$, or $\sigma^0_{LR} < \sigma^0_{RR}$. Both potato and, especially, sugarbeet show an excess of cross-polar return, which implies that the effect of the soil surface at *L* band is still appreciable, possibly through a canopy-terrain interaction. Note that the potato fields, which in figure 2 and 3 clustered together with some tree species, are now distinctly separated.

The final plots report the correlation coefficients ρ (Borgeaud *et al.* 1987, Kong *et al.* 1987), computed through averages over all the pixels belonging to a given field

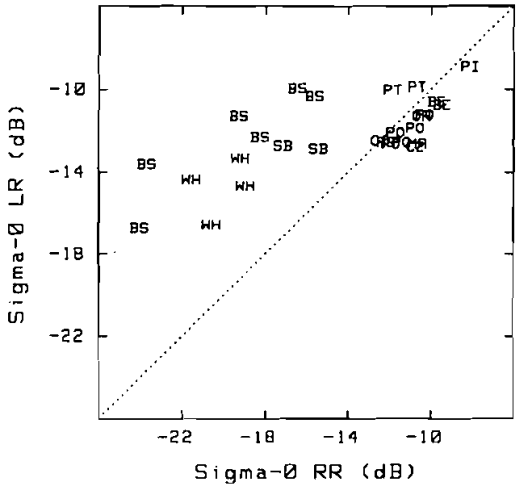

Figure 5. *P* band σ^0_{VV} vs. σ^0_{HH} for some agricultural fields and forest areas in the Flevoland test site. Labels as in figure 2.

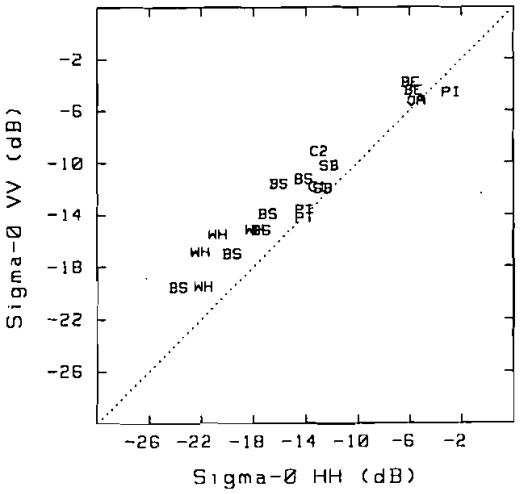

Figure 6. L band left-circular σ^0_{LR} vs. right-circular σ^0_{RR} for some agricultural fields and forest areas in the Flevoland test site. Labels as in figure 2.

or forest stand, plotted in the complex plane at C, L and P band (figure 7). At C band, data relative to all types of surface cluster, so that the identification of distinct trends is difficult. Separation among various classes of response is accomplished at L band. Rough surface scattering by bare soils and wheat is associated with the highest magnitude of ρ and moderately low values of its phase ϕ_ρ. Data of vegetation for which the dominant mechanism is volume scattering are located in the neighbourhood of the real axis, with relatively low values of $|\rho|$. Potato fields, for which scattering is originated mainly by stems and by canopy-terrain interaction, have $|\rho|$ appreciably higher than that of the various trees and normal corn. The points relative to sugarbeet fall in an intermediate region between surface and volume scattering. Indeed, model simulation indicates that, on one side, the soil contribution is appreciable at VV polarization and, on the other, that the interaction between the canopy of leaves and the soil is important at HH. Data for ash, maple and defoliated corn depart from the others, since ϕ_ρ is relatively high. The two types of tree show $|\rho|$ quite close to that of the other stands, while the residual effect of the terrain leads to a slight increase of $|\rho|$ for corn. At P band, the distribution of the data in the complex plane is further different. The data relative to bare soil and wheat, for which we presume a major contribution by surface scattering, are clustered in the neighbourhood of the real axis. The two fields of sugarbeet show relatively high values of both the magnitude and phase of ρ, while the potato fields somewhat depart from the real axis, but have realtively low values of $|\rho|$. Finally, the trees and defoliated corn present the lowest values of $|\rho|$ and high phase (with the exception of one of the beech stands).

3. Conclusions

The MAESTRO I campaign offered a good opportunity to acquire backscattering data useful to progress in the comprehension of the mechanisms that affect the radar return from agricultural fields and forests. In spite of problems, mainly related to RF interferences and calibration uncertainties at P band, an important amount of

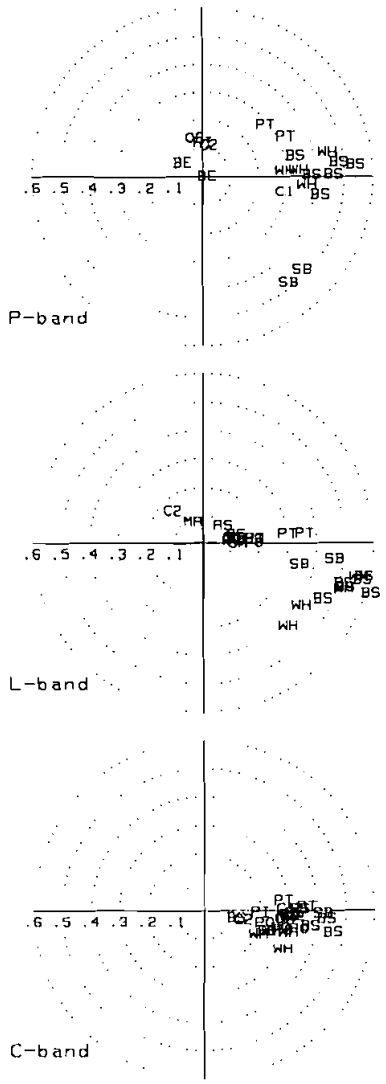

Figure 7. Correlation coefficients at P (top), L (middle) and C band (bottom) for some agricultural fields and forest areas in the Flevoland test site. Labels as in figure 2.

multi-frequency data have been collected, containing significant information on the properties of the electromagnetic interaction with natural surfaces.

Some conclusions can be drawn from the analysis of the polarimetric measurements taken on the Flevoland test site, bearing in mind that only a limited number of agricultural crops and of tree types were considered. At C band, both backscattering coefficients and $HH-VV$ phase differences show a weak dependence on the type of crops and trees; moreover, data for crops overlap those for forest. L band backscattering coefficients vary appreciably both from one crop type to the other and among different species of tree stands. σ^0_{HV} has the highest variation, which reaches about 10 dB between wheat and potato and about 6 dB between maple and

beech. On the other hand, the forest data overlap the crop data. At P band, the sensitivity of σ^0 to crop types is similar; both σ^0_{HH} and σ^0_{VV} have larger variations than those at L band. In addition, unlike L band, a distinct separation (up to about 7 dB) is observed between the most reflective crop (sugarbeet for HH polarization) and the less reflective tree stand (beech, for the same polarization). At L band, the phase difference between VV and HH backscattering does not appear to be sensitive either to the crop or to the tree type, except in particular cases, such as defoliated corn and maple, when some double-bounce scattering mechanism presumably dominates. Phase differences at P band have small (wheat, corn) or moderate (potato, sugarbeet) values for the crops and increase distinctly in the case of trees.

The observed behaviour of the backscattering parameters with both frequency and type of surface can be explained generally on the basis of the scattering mechanisms which settle to produce the radar response, generally in agreement with model results. The P and L band polarization responses of selected agricultural fields appear to hint at the shape and orientation of the main sources of scattering at the respective frequencies. We remark that developed succulent crops do not seem to be transparent at P band, but their structure moulds the corresponding polarization response. Further analysis has been conducted by considering simple plots in planes of pairs of backscattering coefficients, such as the co- and cross-polar linear or circular ones, and in the correlation coefficient complex plane. The synoptic sight offered by such representations gives suggestions on the relative strength of the intervening scattering mechanisms for the various types of crops and trees. Discrimination is not feasible at C band, while L band data localize themselves within regions where either surface or volume scattering prevails, or a double-bounce mechanism intervenes. At the latter frequency, it is noted that the potato plants which behave like a canopy of randomly oriented thin cylinders, are indistinguishable from trees, except at circular polarization. On the other hand, the response of sugarbeet, which can be assimilated to a canopy of relatively large disks, presents some similarity with that of fields with prevailing surface scattering. At P band, the responses of these dense crops tends to merge in the surface scattering region, but their backscattering intensity, which is enhanced with respect to that of the bare soil, and the different $VV-HH$ phase values indicate that they are not quite transparent.

Acknowledgments

This work has been partially supported by ASI, Agenzia Spaziale Italiana. Ground data on the Flevoland test site have been collected by a team from the Agricultural University of Wageningen, The Netherlands (Droesen *et al.* 1990). The authors wish to thank G. de Grandi for his kind co-operation.

References

BORGEAUD, M., KONG, J. A., and SHIN, R. T., 1987, Theoretical models for polarimetric radar clutter. *Journal of Electromagnetic Waves and Applications*, **1**, 73–89.

CHAUHAN, N. S., LANG, R. H., and RANSON K. J., 1991, Radar modeling of a boreal forest. *I.E.E.E. Transactions on Geoscience and Remote Sensing*, **29**, 627–638.

CHURCHILL, P. N., and ATTEMA, E. P. W., 1991, The European airborne polarimetric SAR campaign MAESTRO-1. *Proceedings of IGARSS'91, Espoo, Finland, 3-6 June 1991*, I.E.E.E. 91CH2971-0 (New York: The Institute of Electrical and Electronics Engineers), pp. 327–328.

CUMMING, I. G., SMALL, D. L., and VAN ZYL, J. J., 1991, Information content of polarimetric SAR data. *Proceedings of the Third Airborne Synthetic Aperture Radar (AIRSAR) Workshop, Pasadena, CA, U.S.A., 1 August 1991*, JPL publication 91-30 (Pasadena, CA: Jet Propulsion Laboratory), pp. 177–186.

DE MATTHAEIS, P., FERRAZZOLI, P., SCHIAVON, G., and SOLIMINI, D., 1992 a, AGRISCATT and MAESTRO: Multifrequency radar experiments for vegetation remote sensing. *Proceedings of the MAESTRO-1/AGRISCATT Workshop, ESTEC, Noordwijk, The Netherlands, 6–7 March 1992*, ESA WPP-31 (Paris: European Space Agency), pp. 231–248.

DE MATTHAEIS, P., FERRAZZOLI, P., SCHIAVON, G., and SOLIMINI, D., 1992 b, Analysis of scattering features of forests and agricultural areas. *Proceedings of the URSI Microwave Signature Conference, Igls, Austria, 1–3 July 1992* (Oberpfaffenhofen, Germany: Deutsche Forschungsanstalt für Luft- und Raumfahrt), pp. 2B22–2B26.

DOBSON, M. C., ULABY, F. T., LE TOAN, T., BEAUDOIN, A., KASISCHKE, E. S., and CHRISTENSEN, N., 1992, Dependence of radar backscatter on coniferous forest biomass. *I.E.E.E. Transactions on Geoscience and Remote Sensing*, **30**, 412–415.

DROESEN, W. J., HOEKMAN, D. K., VAN LEEUWEN, H. J. C., VAN DER SANDEN, J. J., BOUMAN, A. M., UENK, D., VISSERS, M. A. M., and LEMOINE, G. G., 1990, MAESTRO 89 ground data collection Horsterwold/Speulderbos/Flevoland, Technical Report Wageningen Agricultural University, The Netherlands.

DURDEN, S., FREEMAN, A., KLEIN, J., VANE, G., ZEBKER, H., ZIMMERMANN, R., and OREN, R., 1991, Polarimetric radar measurements of a tropical rain forest. *Proceedings of the Third Airborne Synthetic Aperture Radar (AIRSAR) Workshop, Pasadena, CA, U.S.A., 1 August 1991*, JPL publication 91-30 (Pasadena, CA: Jet Propulsion Laboratory), pp. 223–229.

DURDEN, S. L., VAN ZYL, J. J., and ZEBKER, H. A., 1989, Modeling and observation of the radar polarization signature of forested areas. *I.E.E.E. Transactions on Geoscience and Remote Sensing*, **27**, 290–301.

EVANS, D. L., FARR, T. G., VAN ZYL, J. J., and ZEBKER, H. A., 1988, Radar polarimetry: analysis tools and applications. *I.E.E.E. Transactions on Geoscience and Remote Sensing*, **26**, 774–789.

FERRAZZOLI, P., GUERRIERO, L., and SOLIMINI, D., 1991, Numerical model of microwave backscattering and emission from terrain covered with vegetation. *Applied Computational Electromagnetics Society Journal*, **6**, 175–191.

FERRAZZOLI, P., and GUERRIERO, L., 1994, Interpretation and model analysis of MAESTRO 1 Flevoland data. *International Journal of Remote Sensing*, **15**, 2901–2915.

FORSTER, R. R., FOX, A. N., and ISACKS, B., 1992, Preliminary results of polarization signatures for glacial moraines in the Mono basin, eastern Sierra Nevada. *Summaries of the Third Annual JPL Airborne Geoscience Workshop, Pasadena, CA, U.S.A., 1–5 June 1992*, JPL publication 92-14, Volume 3, edited by J. J. van Zyl (Pasadena, CA: Jet Propulsion Laboratory), pp. 40–42.

FREEMAN, A., VILLASENOR, J., and KLEIN, J. D., 1991, Multi-frequency and polarimetric radar backscatter signatures for discrimination between agricultural crops at the Flevoland experimental test site. *Proceedings of the Third Airborne Synthetic Aperture Radar (AIRSAR) Workshop, Pasadena, CA, U.S.A., 1 August 1991*, JPL publication 91-30 (Pasadena, CA: Jet Propulsion Laboratory), pp. 44–56.

FRENCH, N. H. F., BOURGEAU-CHAVEZ, L. L., KASISCHKE, A. E., and SHEEN, D. R., 1991, Analysis of polarimetric SAR signatures of vegetated areas. *Proceedings of the Third Airborne Synthetic Aperture Radar (AIRSAR) Workshop, Pasadena, CA, U.S.A., 1 August 1991*, JPL publication 91-30 (Pasadena, CA: Jet Propulsion Laboratory), pp. 22–33.

GROOT, J. S., VAN DER BROEK, A. C., and FREEMAN, A., 1992, An investigation of the potential of polarimetric SAR data for discrimination between agricultural crops. *Proceedings of the MAESTRO-1/AGRISCATT Workshop, ESTEC, Noordwijk, The Netherlands, 6–7 March 1992*, ESA WPP-31 (Paris: European Space Agency). pp. 67–82.

HELD, D. H., BROWN, W. E., FREEMAN, A., KLEIN, J. D., ZEBKER, H., SATO, T., NGUYEN, Q., and LOU, Y., 1988, The NASA/JPL multifrequency, multipolarization airborne SAR system. *Proceedings of IGARSS'88, Edinburgh, U.K., 12–16 September 1988*, ESA SP-284 (Paris: European Space Agency), pp. 345–349.

KARAM, M. A., FUNG, A. K., LANG, R. H., and CHAUHAN, N. S., 1992, A microwave scattering model for layered vegetation. *I.E.E.E. Transactions on Geoscience and Remote Sensing*, **30**, 767–784.

KONG, J. A., SWARTZ, A. A., YUEH, H. A., NOVAK, L. M., and SHIN, R. T., 1987, Identification of terrain cover using the optimum polarimetric classifier. *Journal of Electromagnetic Waves and Applications*, **1**, 171–193.

MCDONALD, K. C., DOBSON, M. C., and ULABY, F. T., 1991, Modeling multifrequency diurnal backscatter from a walnut orchard. *I.E.E.E. Transactions on Geoscience and Remote Sensing*, **29**, 853–863.

MO, T., WANG, J. R., and ENGMAN, E. T., 1990, SAR polarization signatures of natural fields. *Proceedings of IGARSS'90, Washington, D.C., U.S.A., 20–24 May 1990*, I.E.E.E. 90CH2825-8 (New York: The Institute of Electrical and Electronics Engineers), pp. 1679–1682.

RAY, T. W., FARR, T. G., and VAN ZYL, J. J., 1991, Polarization signatures for abandoned agricultural fields in the Manix basin area of the Mojave desert. *Proceedings of the Third Airborne Synthetic Aperture Radar (AIRSAR) Workshop, Pasadena, CA, U.S.A., 1 August 1991*, JPL publication 91-30 (Pasadena, CA: Jet Propulsion Laboratory), pp. 117–125.

SKRIVER, H., and GUDMANDSEN, P., 1992, Analysis of MAESTRO-1 polarimetric SAR data of forest areas at Les Landes. *Proceedings of the MAESTRO-1/AGRISCATT Workshop held at ESTEC, Noordwijk, The Netherlands, 6–7 March 1992*, ESA WPP-31 (Paris: European Space Agency), pp. 131–136.

TSANG, L., and DING, K. H., 1991, Polarimetric signatures of a layer of random nonspherical discrete scatterers overlying a homogeneous half-space based on first- and second-order vector radiative transfer theory. *I.E.E.E. Transactions on Geoscience and Remote Sensing*, **29**, 242–253.

ULABY, F. T., SARABANDI, K., MCDONALD, K., WHITT, M., and DOBSON, M. D., 1990, Michigan microwave canopy scattering model. *International Journal of Remote Sensing*, **11**, 1223–1253.

VAN ZYL, J. J., 1989, Unsupervised classification of scattering behavior using radar polarimetric data. *I.E.E.E. Transactions on Geoscience and Remote Sensing*, **28**, 36–45.

VAN ZYL, J. J., 1990, Calibration of polarimetric radar images using only image parameters and trihedral corner reflector responses. *I.E.E.E. Transactions on Geoscience and Remote Sensing*, **28**, 337–347.

VAN ZYL, J. J., DUBOIS, P., and GUERRA, A., 1991, Monsoon '90: Preliminary SAR results. *Proceedings of the Third Airborne Synthetic Aperture Radar (AIRSAR) Workshop, Pasadena, CA., U.S.A., 1 August 1991*, JPL publication 91-30 (Pasadena, CA: Jet Propulsion Laboratory), pp. 88–97.

VAN ZYL, J. J., and ULABY, F. T., 1990, Scattering matrix representation for simple targets. In *Radar Polarimetry for Geoscience Applications*, edited by F. T. Ulaby and C. Elachi (Norwood, MA: Artech House), pp. 17–52.

VAN ZYL, J. J., ZEBKER, H. A., and ELACHI, C., 1987, Imaging radar polarization signatures: Theory and observation. *Radio Science*, **22**, 529–543.

ZEBKER, H. A., and LOU, Y., 1990, Phase calibration of imaging radar polarimeter Stokes matrices. *I.E.E.E. Transactions on Geoscience and Remote Sensing*, **28**, 246–252.

ZEBKER, H. A., VAN ZYL, J. J., DURDEN, S. L., and NORIKANE, L., 1991, Calibrated imaging radar polarimetry: Technique, examples, and applications. *I.E.E.E. Transactions on Geoscience and Remote Sensing*, **29**, 942–961.

ZEBKER, H. A., VAN ZYL, J. J., and HELD, D. N., 1987, Imaging radar polarimetry from wave synthesis. *Journal of Geophysical Research*, **92**, 683–701.